Log-normal distributions of suspended particles in the open ocean

by Claude E. Lambert,[1] C. Jehanno,[1] N. Silverberg,[2] J. C. Brun-Cottan[3] and R. Chesselet[1]

ABSTRACT

A scanning electron microscope-electron microprobe technique was used to chemically distinguish and size particles as fine as 0.2μm on GEOSECS suspended matter filters from the open ocean.

The populations of aluminosilicate, silica, iron oxide, as well as aggregate particles were found to follow a log-normal size distribution. Organic particles show a similar, but imperfect, log-normal distribution.

The absolute concentrations of aluminum, measured by instrumental neutron activation analysis, together with the parameters of the log-normal distribution have yielded an estimate of 10-30 μg/cm^2/yr for the flux of fine particles of aluminosilicate to the sea floor, with settling velocities of 30-150 m/yr. This population has thus a long residence time in the open ocean.

Other sources, very probably the much larger, fast-settling fecal material, and near-bottom horizontal mass transport of material from the continental margins, provide the bulk of sedimentary aluminosilicates.

1. Introduction

Knowledge of particle size distribution, and hence mass, settling velocity and transport behavior, is of increasing concern in marine geochemistry as the role of suspended particles in the ocean becomes better known. The chemical balances of many substances in the ocean appear to be controlled by cycles involving the particulate phase (Boyle *et al.*, 1977; Turekian, 1977; Sclater *et al.*, 1976; Bruland *et al.*, 1978; Buat-Menard and Chesselet, 1979).

However, no adequate description exists for suspended particles over a broad range of particle sizes. Approaches using water bottle samples are limited to the fine fraction (less than about 50 μm) since coarser particles are very inefficiently sampled, while recently developed methods of sampling the coarse fraction (large

1. Centre des Faibles Radioactivités, CFR, Laboratoire Mixte CNRS-CEA, Gif-sur-Yvette, F 91190 France.

2. Centre des Faibles Radioactivités, on sabbatical leave from Université du Québec à Rimouski, Qué., Canada.

3. Laboratoire de Physique et de Chimie marines, Université Pierre et Marie Curie, Paris, France.

volume filtration or sediment traps) tend to render the fine fraction unanalyzable due to loss within the filters or coagulation.

A power law distribution, with the number of particles increasing with decreasing grain size, is currently in preferred usage. This is based upon studies by Junge (1963), who described such a function for airborne particulate matter. Coulter counter analyses of water bottle samples by Bader, 1970; Brun-Cottan, 1971, 1976a; Lerman *et al.*, 1977 and others have produced many size distributions for marine suspended matter which appear to follow the same function. Harris (1977) has directly measured particles as small as 0.02 μm on filters from the ocean by means of transmission electron microscopy, and also reports a power distribution. Power function parameters were used to describe the only available measurements of the size distribution for coarse particles (Bishop *et al.*, 1977, 1978), on samples obtained by large volume filtrations.

If the geochemistry of specific components is to be separated from the behavior of the mass, it is necessary to obtain information about the size distribution of individual components. By using a multiple technique approach: chemical identification and sizing of particles using scanning electron microscopy and electron microprobe (SEM-EMP) and precise bulk chemical analyses using instrumental neutron activation analysis (INAA), researchers at the Centre des Faibles Radioactivités have succeeded in describing size distributions and fluxes for individual components such as calcium carbonate (Aubey, 1976; Aubey and Chesselet, 1977), barite (Dehairs *et al.*, 1980) and ferric hydroxides and oxides (Lambert, 1979).

In this study, we used this coupled approach to elucidate the size distribution of several other components, principally aluminosilicates, in GEOSECS water bottle samples obtained from deep and bottom waters from different parts of the world ocean.

Because of the geographic and temporal variability of biological activity, we have decided not to include surface water samples in this presentation. From the geochemical point of view the complex surface layer can be considered as a "black box" which receives inputs from different sources and attains an internal equilibrium with respect to the passage of particles to the subsurface waters (Buat-Menard and Chesselet, 1979).

2. Methods and procedures

a. Sampling. The sampling procedures used are those which were standardized for the GEOSECS program and are described in detail in Brewer *et al.*, 1976. Extensive studies showed that the 0.4 μm Nuclepore filters very efficiently trap even the smallest particles (0.1 μm) examined. The number of particles in the 0.1-0.4 μm size range retained on 0.2 and 0.1 μm porosity filters placed in line, amounted to less than 5% of the number retained on the original 0.4 μm filter. Other tests were

made to see if the filter samples were biased because of large particles which may have quickly settled to the bottom of the Niskin bottles and thus were not sampled at the level of the sampling spigot (Gardner *et al.*, 1976). These tests confirmed that such a bias is detectable only for surface and near bottom water samples, which include significant proportions of large grains.

b. SEM-EMP. Each pre-weighed 0.4 μm Nuclepore filter (Brewer *et al.*, 1976), was cut into quarters (2.5 cm^2) for different analyses. A portion of one quarter (1-2 cm^2) was mounted on a stub, coated under vacuum with 0.02 μm carbon, and examined using a CAMECA electron microscope (SEM) coupled with an EDAX energy dispersive X-ray spectrometer (EMP). A magnification of 5000× was used in examining particles from different fields over the available filter surface to obtain representative counts. For each field, every particle encountered was examined by EMP to ascertain the elements present. The diameter for spheroidal grains, or the long and intermediate dimensions, for nonspheroidal grains, were measured directly for each particle which contained both Al and Si (some data will also be presented for Fe and Si particles). For the Nuclepore filters and the instrumentation used, the smallest diameter that could be investigated was 0.1 μm.

The method is very time consuming but it is the only one available which both identifies and measures particles in the sub-micrometer range. Because of budget and time considerations, a total of 100-500 individual aluminosilicate particles and 50-200 complex aluminos-silicate bearing aggregate particles were counted for each sample. Separate, repeated 100 particle-counts for given filters confirmed the reliability of the method.

The data were then plotted on log-probability paper to study the size distributions. For non-spherical particles, D^*, the diameter of a circle having the same projected area as the particle, was used. We estimate the overall precision of the particle diameter as $\pm$ 0.1 μm for particles < 5 μm and $\pm$ 0.5 μm for particles > 5 μm.

c. INAA. For each sample, one of the quarter-filters was pelletized, then irradiated for 4 minutes in the EL 3 reactor (Saclay, France) at a flux of 3×10^{12} neutrons/cm^2/sec. The Al was calculated from the transformation $^{27}Al\ (n, \gamma) \rightarrow {}^{28}Al$ ($T = 2.3$ min) using a 110 cm^3 Ge(Li) detector 3 to 4 minutes after irradiation.

3. General description of the particles studied

The particulate material is generally evenly dispersed over the Nuclepore membrane surface and the density is low, so that individual particles are easily distinguished. A diverse population of particles is present, consisting of recognizable skeletal fragments of coccoliths, diatoms and radiolarians, aluminosilicate grains, quartz grains, metal oxides and various kinds of aggregate grains and organic particles (Plate 1).

a

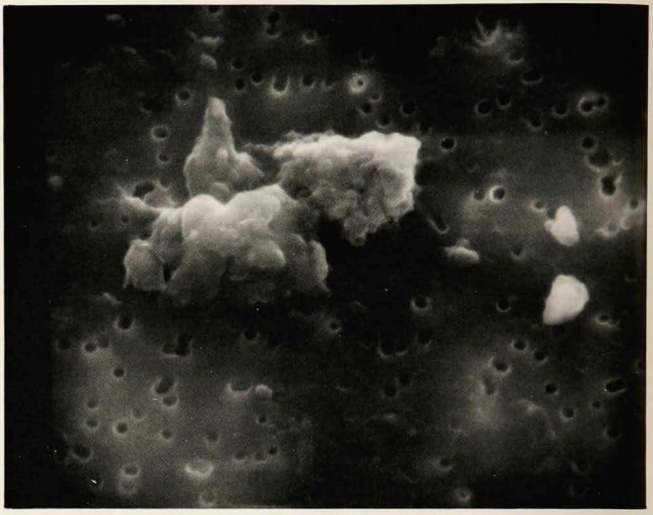

b

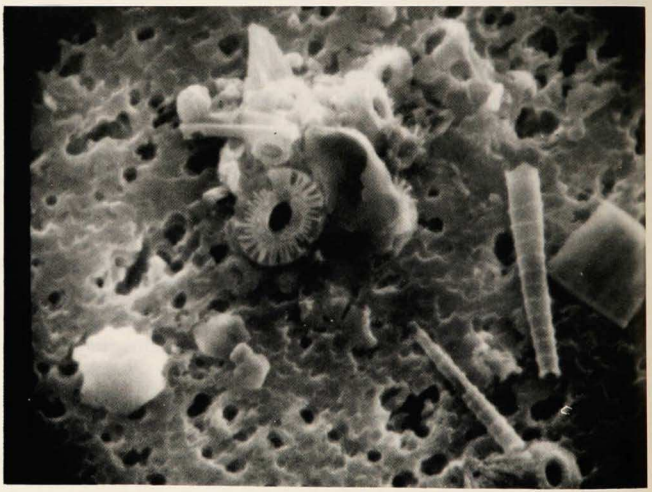

Plate 1. Diversity of particles encountered on the filters.
a) large organic-rich plus small Fe-rich.
b) skeletal debris, mineral grains and organic particles.

a

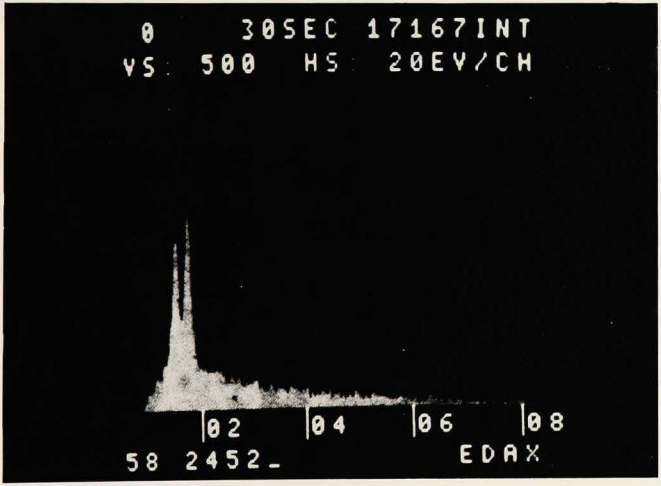

b

Plate 2. Large aluminosilicate particle and 3 small quartz grains.
b) Edax spectrum of aluminosilicate particle showing the Al peak on the left and the Si peak to the right.

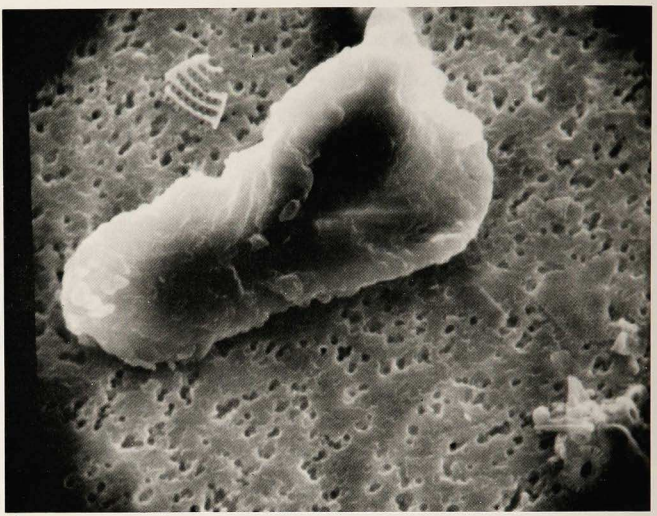

Plate 3. Organic aggregate.

Aluminosilicate particles: these particles are all finer than about 10 μm in size. They vary in form from spherical to highly irregular and most have good relief, indicating considerable thickness. They are identified by clear Al-Si signals and Fe, K, Na, Ca, Mg responses are often evident as well (Plate 2).

Quartz grains: these particles are rare and occur essentially in the fine fraction. They are generally equant in form and give strong Si EMP signals without Al.

Opaline fragments: these are distinguished from quartz grains by their fragmental form and weak Si signal. Such distinctions become unusable for sizes finer than about 1 μm.

Aggregates: Virtually all of the particles coarser than about 10 μm were distinctly composite. Shapes tend to be highly irregular and variable. Three principal types of aggregates can be discerned:

a. organic aggregates: These usually have well defined borders and forms, with a mostly homogeneous appearance, and elicit very low EMP counting rates, only slightly above the blank Nuclepore filter surface. They display no specific element response, or only S and Cl with some traces of Ca, P or Fe. Very often, however, a few aluminosilicate or Fe-rich particles are detectable within the otherwise organic masses (Plate 3).

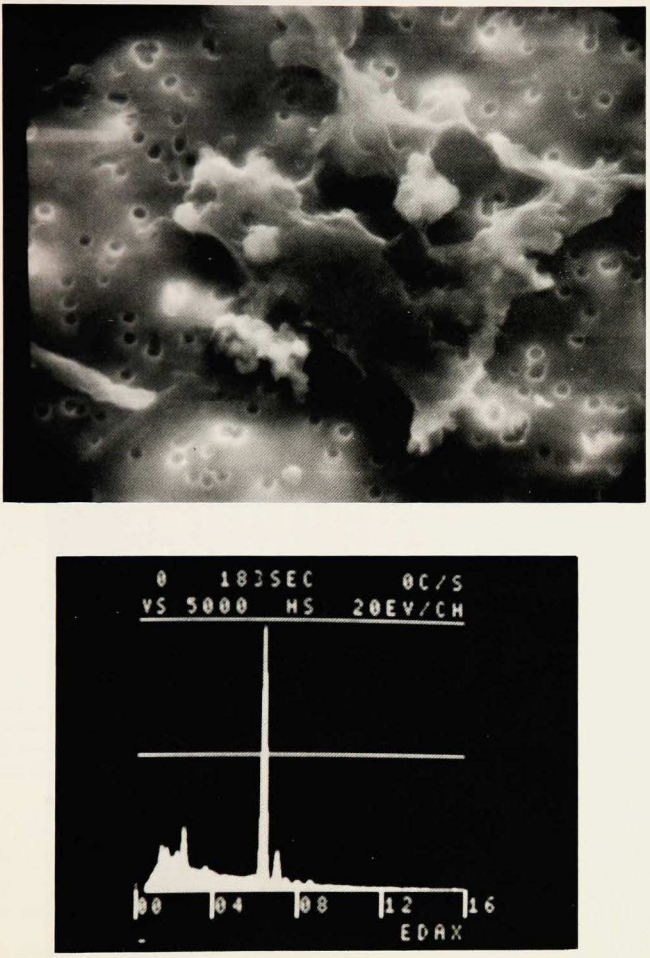

Plate 4.
a) Heterogeneous aggregate with Fe-rich inclusions.
b) Edax spectrum showing strong Fe peak.

a

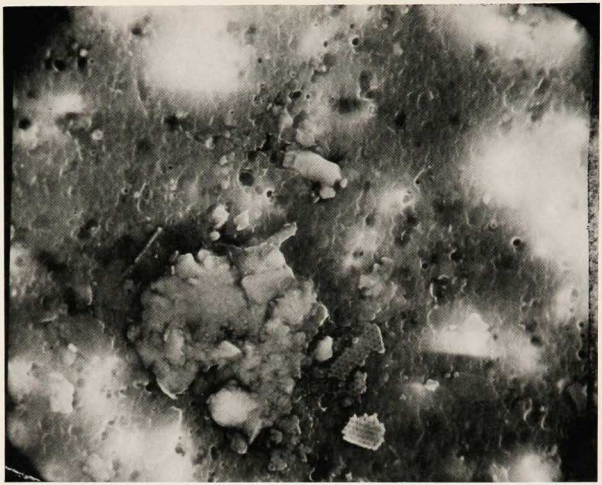

b

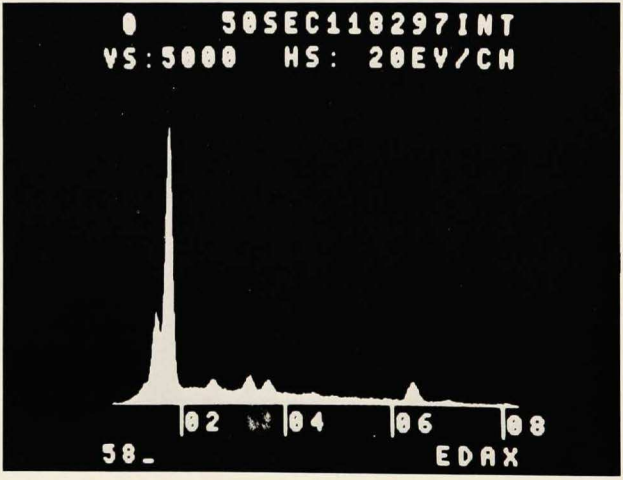

Plate 5.

a) Large aluminosilicate aggregate.

b) Typical spectrum showing strong Al and Si peaks with peaks of K, Ca and Fe.

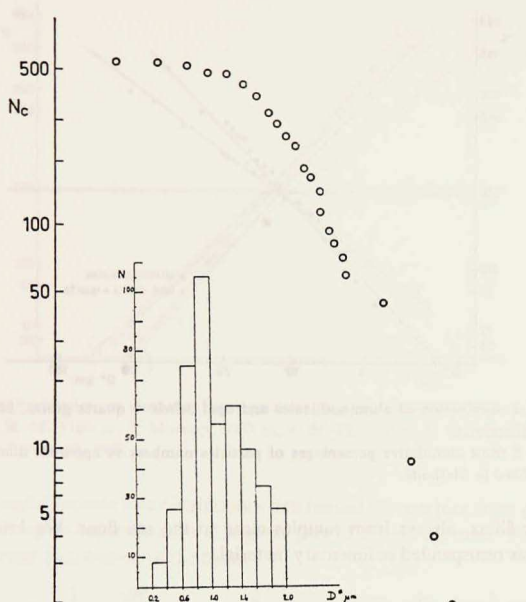

Figure 1. Size distribution of aluminosilicate particles St. 58, 4424 m (log log scale) Nc is the number of particles for which the diameter $>D^*$. In the lower left-hand corner of this figure, we show the particles-sizes *histogram* for this sample number of observed particles vs their sizes-class ranking).

b. heterogeneous aggregates: These grains contain at least 3 compounds, generally organic matter, aluminosilicate and skeletal fragments. Oxides of Fe, Ti or barite crystals may also be present. Although these aggregates most likely represent fecal material, their form is open and porous and not "pellet-like" (Plate 4).

c. Aluminosilicate aggregates: Unlike the 2 other kinds of aggregates, this type (Plate 5) does not appear to be of biogenic origin. They have a characteristic shape, platey and flaky in appearance, and aluminosilicates (Al, Si, K, Ca, Fe) account for about 90% of the component grains They have been encountered on 20 Atlantic

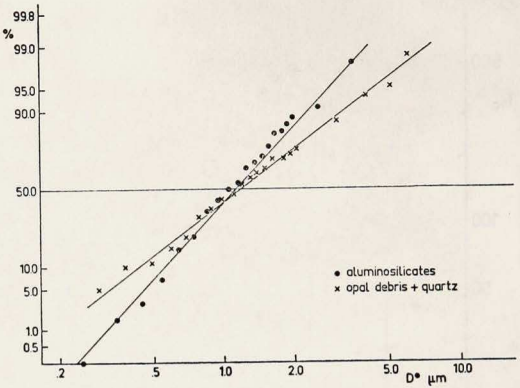

Figure 2. Size distribution of aluminosilicates and opal debris + quartz grains, St. 58, 4424 m (log normal scale).

Figures 2 to 8 show cumulative percentages of particles numbers vs apparent diameter (D^*, in μm) as defined in Methods.

and Pacific filters, always from samples close to the sea floor. We interpret these aggregates as resuspended sedimentary material.

4. Size distributions of aluminosilicate particles

Figure 1 shows the size distribution for GEOSECS Atl.st.58, 4422 m, for which 500 individual grains were counted. The data is plotted on a log-log scale, in conformity with the conventions currently used for size distributions, but it is obvious that the distribution does not follow a power function. Most interestingly, the position of the inflection point, where the curve begins to flatten out, corresponds to a diameter of 0.8 μm. This is just below the limit of functional Coulter counter analysis. The distribution presented here is in fact log-normal as is also demonstrated in Figure 2, where the same data are plotted on a log-probability graph.

The basic difference between the two functions is that for the log-normal distribution a peak occurs in particle numbers (see inset Fig. 1) while for the power function, particle numbers continue to increase with diminishing grain sizes. For the portion of the size distribution coarser than the peak size, the log-normal and power functions are both straight line plots and are essentially indistinguishable. The concordance with the straight line behavior of log-normal distributions on this type of plot (Fig. 2) is excellent (correlation coefficient 0.996). On this figure we include the size distribution for silica (opal + quartz particles) from the same sample, to show that these particles also follow a very similar log-normal distribution.

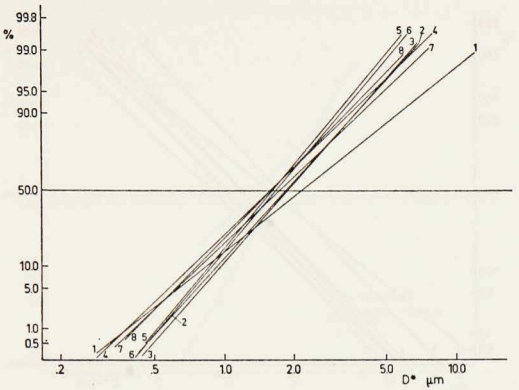

Figure 3. Size distribution of aluminosilicate particles (log normal scale) *Atlantic*: 1: St. 58, 4424 m; 2: St. 58, 3100 m; 3: Madcap, 2000 m; 4: St. 82, 286 m; 5: St. 67, 2391 m; 6: St. 91, 2002 m; 7 = St. 67, 1953 m.

Figures 3 and 4 include size distributions determined for samples from geographic positions and depths representative of a great part of the open ocean. They all follow a log-normal distribution of the form:

$$y = \frac{1}{N}\frac{dN}{dD^*} = \frac{1}{\sigma\sqrt{2\pi}D^*}\exp\left(-\frac{1}{2}u^2\right)$$

where y is a function of 2 parameters: u and σ, and where $u = \dfrac{\ln D^* - L}{\sigma}$ follows the normalized Laplace-Gauss function with:

$$Y(D^*) = \int_0^{D^*} y\, dD^*$$

$Y(D^*)$ is normalized following $Y = \int_0^{\infty} y\, dD^* = 1$

$L = \ln D^*_m$, D^*_m is the diameter corresponding to the median. σ is the standard deviation of u following the Laplace-Gauss function.

Table 1 lists the χ^2 goodness of fit (to a log-normal distribution) for these samples, as well as the general parameters (mean diameter, median, and σ).

The χ^2 test is extremely sensitive to variations at the tails of the size distributions. If the small number of particles detected at the extremes are eliminated, the χ^2 values become very good (values in parentheses, Tables 1, 5). This suggests that a small, coarser-grained, secondary population may exist for certain samples.

The curves show that the size distributions of aluminosilicate particles over the

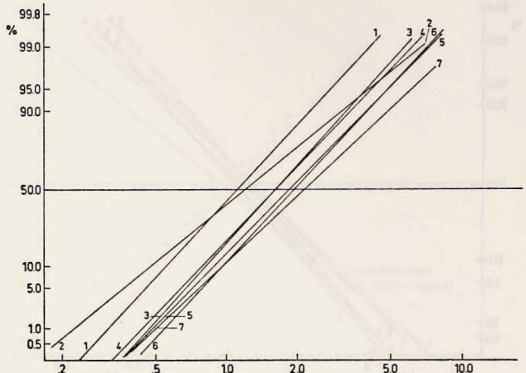

Figure 4. Size distribution of aluminosilicate particles (log normal scale) *Pacific*: 1: St. 257, 2814 m; 2: St. 306, 2458 m; 3: St. 306, 3564 m; 4: St. 306, 3693 m; 5: St. 306, 3879 m; 6: St. 306, 4278 m; 8: St. 306, 5474 m.

Table 1. Size distribution of aluminosilicates.

Station	Point	Depth (m)	$\bar{D}^*$ μm	D^*_m μm	σ	X^2 significant level	
			Atlantic				
58	27°00 S-37°00 W	3100	1.5	1.2	0.71	.005	
		4424	1.5	1.1	0.54	.005	
67	44°59 S-51°10 W	1958	2.5	2.1	0.62	.005	
		2391	2.3	1.9	0.58	.25	
82	56°16 S-24°55 W	286	1.4	1.6	0.58	.005	
91	49°34 S-11°28 E	2002	1.8	1.9	0.56	.995	(.005)
MADCAP	28°40 N-25°25 W	2000	1.3	1.6	0.52	.005	
			Pacific				
257	10°10 S-170°00 W	2814	2.5	2.1	0.64	.005	
306	32°49 S-163°32 W	2458	3.6	1.9	0.52	.025	
		3564	3.1	1.9	0.52	.995	(.025)
		3693	2.3	1.6	0.61	.995	(.05)
		3879	1.8	1.6	0.50	.005	
		4079	1.7	1.7	0.49	.25	
		4278	1.8	1.7	0.62	.005	
		5474	1.8	1.6	0.56	.005	

$\bar{D}^*$ mean diameter
D^*_m median diameter
σ standard deviation of the log of D^*_m: $ln\left(\frac{D^*.842}{D^*_m}\right)$

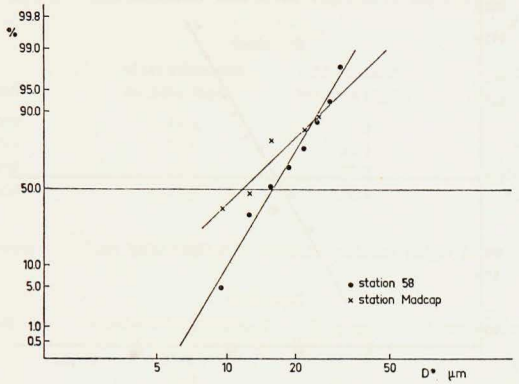

Figure 5. Size distribution of aggregates (8-30 μm), St. 58, 4424 m; St. Madcap, 2000 m.

entire open ocean fall within a very limited number of families. The overall variation in mean size is not large (range 1 μm to 3 μm).

5. Size distribution of aggregate particles

As indicated in the description of the types of particles, aggregate particles dominate the size classes coarser than about 10 μm and parametrization of their sizes involves some degree of error. Figure 5 shows the determined size distributions for 2 samples. To obtain a better view of the size distribution of these aggregates, we have combined data from several samples to produce a generalized distribution (Fig. 6). The straight line relationship is much better defined.

6. Representativity of the SEM-EMP data

Implicit in the usage of ultrafine approaches such as high magnification scanning electron microscopy is the hazard of "missing the forest for the trees". The facts that: only several hundred or even several thousand grains out of several million could be examined; that only an essentially two-dimensional measure is possible on a flat viewing screen (although depth of field is excellent with SEM); and that many particles are irregularly shaped and must be parametrized by equivalent diameters, requires that some tests be made of the representativity of the microscope data with respect to the bulk sample.

The total Al content on the filters as measured by INAA, is a precise bulk measurement. If we can show that the individual particle counts can reproduce this

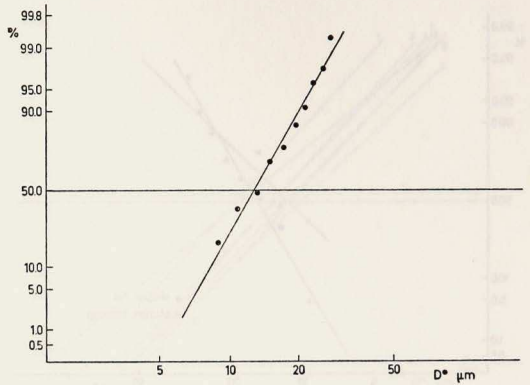

Figure 6. Generalized distribution of aggregates (8-30 μm) for 5 different depths at St. 58.

bulk measurement, then we can trust that the SEM-EMP data is representative. To correct the size data to mass data, we have used the following method:

By integrating the first order moment of the log-normal size distribution using theorems 2-1 and 2-2 of Aitchinson and Brown (1976), we obtain the mean particle volume (Brun-Cottan, to be published)

$$\bar{v} = \frac{\pi}{6} \exp\left(3L + \frac{9}{2} \sigma^2 \right)$$

Knowing the area of the filter and the number of particles counted, as well as the volume of water filtered, we can calculate the number of aluminosilicate particles per ml of seawater. The density of these particles cannot be measured directly. We assume for the low-temperature-dried filters (to compare with the INAA calculations) a density of 2 g/cm^3. Finally, we use the value of 10% as representative of the overall proportion of Al in marine aluminosilicates. The general equation is thus:

$$\text{Mass Al/ml filtered} = 0.1\, N\, \bar{v}\, \rho$$

where 0.1 = proportion of Al in aluminosilicate particles; N = number of particles per ml; ρ = dry density; $\bar{v}$ = mean particle volume. Since this equation assumes that all the particles are spheres, the mass must be corrected for those particles which are not spheres. We have calculated the proportion (%) of such particles and estimate that their mass volume is one half that of spheroidal particles. Table 2 shows the data calculated for 4 different filters.

To arrive at the total mass of Al, the contribution of Al by aggregate particles must be included. Because of the irregularity of these grains the size measurements

Table 2. Computation from SEM-EMP data of the weight of Al supported by aluminosilicate particles.

	Station 58		
Depth	Al on spheroidal particles (ng/1)	Al on other particles (ng/1)	Total Al on particles (ng/1)
279	35.9	17.9	53.8
2088	33.5	39.1	72.6
3100	50.7	59.2	109.0
4424	238.4	278.1	516.5

Table 3. Computation from SEM-EMP data of aluminosilicate weight in heterogeneous aggregates.

	Station 58		
Depth (m)	Number of aggregates/1	$\bar{D}$* (μm)	Aluminosilicate content
279	3000	15	1- 2%
2088	1440	15	10-20%
3100	1300	15	10-20%
4424	3900	18	40-80%
	Aluminosilicate aggregates		
4424	300	20	90%

Table 4. Comparison of total weight of Al (ng/1 of seawater) computed from SEM-EMP data with total Al (ng/1 of seawater) INAA data.

Depth	Particles SEM-EMP	Aggregates SEM-EMP	Total SEM-EMP	Total INAA
279	53.8	2-4	56-58	85
2088	72.6	19-39	92-112	140
3100	109.9	18-35	128-145	140
4424	516.5	368-671*	885-1187	1010

* Including 65 ng/1 of Al from pure aluminosilicate aggregates (resuspension in the upper nepheloid).

are less meaningful and the mean volumes cannot be easily computed from the size distribution. Instead, direct measures of aggregate particle diameters were used. A mean thickness of 3 μm was applied to the aggregates, based upon observations of vertically oriented coccoliths, to calculate volumes, and the volume of each aggregate was corrected for the observed proportion of aluminosilicate particles within the aggregate. These calculations are subject to much greater errors than those for the mass distribution of the individual particles and the results given in Table 3 reflect the probable range (factor of 2) of the weights of Al carried as aggregates for each sample.

Table 5. Size distribution of other classes of particles.

Station	Point	Depth (m)	$\bar{D}^*$ μm	D^*_m μm	σ	X^2 significant level	
			Goethite Particles (FeOOH)				
306(PAC)	32°49 S-163°32 W	2458	1.4	1.2	0.60	.005	
		3879	1.2	1.0	0.59	.25	
		4079	1.8	1.2	0.53	.005	
			SiO_2 Particles				
58(ATL)	27°00 S-37°00 W	4424	1.8	1.3	0.81	.005	
306(PAC)	32°49 S-163°32 W	2458	2.0	1.3	0.28	.005	
		3879	2.4	1.1	0.22	.005	
			Organic Particles				
306(PAC)	32°49 S-163°32 W	2458	3.3	1.7	0.24	.005	
		3564	4.1	1.4	0.25	.025	
		3783	2.4	1.3	0.23	.005	
		3879	3.1	1.3	0.24	.995	(.005)
			Aggregates (8μm-30 μm)				
MADCAP	28°40 N-25°25 W	2000	17.5	11.5	0.58	.005	
67(ATL)	44°59 S-51°10 W	2391	20.6	16.0	0.54	.005	
58(ATL)	27°00 S-37°00 W	4424	20.0	16.0	0.54	.005	
58(ATL)	27°00 S-37°00 W	below 2000	17.8	13.0	0.33	.005	

$\bar{D}^*$ mean diameter
D^*_m median diameter
σ standard deviation of the log of D^*_m

The comparison in Table 4 between the total concentration of Al calculated in the above manner from the SEM-EMP data and the values obtained by INAA is surprisingly good, considering all the assumptions and approximations of the procedure. These tests confirm the representativity and reliability of the electron microscope approach.

7. Other components

The size distribution for silica (opaline fragments and quartz grains) are presented in Figure 1 and that for Fe-oxide in Figure 7. These are also log-normal, with parameters listed in Table 5. A typical plot for organic particles and another for total particulates for the same sample are shown in Figure 8. Although the χ^2 test values admit agreement with log-normality, it is apparent that organic debris depart somewhat from log-normality and influence the size distribution of samples with abundant organic particles.

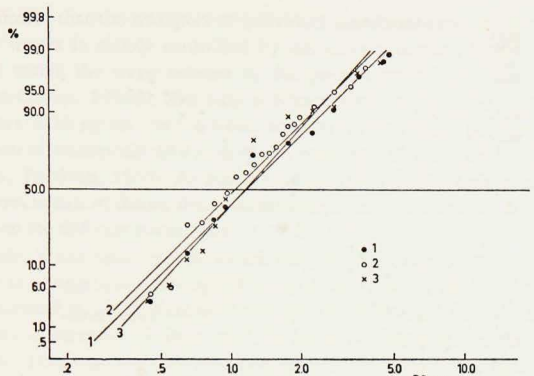

Figure 7. Size distribution of goethites (FeOOH) at St. 306. 1 = 2458 m; 2: 3879 m; 3: 4079 m.

8. Flux calculations of aluminosilicates

The log-normal distribution of the aluminosilicate particles makes the task of calculating the downward flux realistic, since mean parameters can be used to describe the total population of particles. Thus, if the mass flux for a given particle diameter is given by:

$$d\Phi = dN \frac{\Pi}{6} D^3 \quad \rho_d \times C\, D^2 \left(\frac{\rho_p - \rho_w}{\rho_w} \right)$$

mass conc. × settling velocity

where N = total number of particles/unit volume; ρ_d = dry density of the sphere; 2.0 g/cm³; ρ_p = wet density of the sphere in seawater : 1.6 g/cm³; ρ_w = density of the water : ~ 1 g/cm³; D = particle diameter; $C = \frac{1}{18} \frac{g}{\nu}$ (g = gravitation acceleration : 981 cm/s²; ν = kinematic viscosity ~1.5×10^{-2} cm²/s). Then, upon integration, a total mass flux, Φ, can be obtained for the log-normal size distribution (Brun-Cottan, to be published) : $\Phi = \int_0^\infty d\Phi$

$$\Phi = N \frac{\Pi}{6} C \exp\left(5\, L + \frac{25}{2} \sigma^2 \right) \rho_d \frac{\rho_p - \rho_w}{\rho_w}$$

We apply a correction to take account of the percentage of those particles which are not spheroidal by again applying the half-sphere mass correction factor of 0.5 and a correction for the nonspherical shape in the settling velocity term. For the

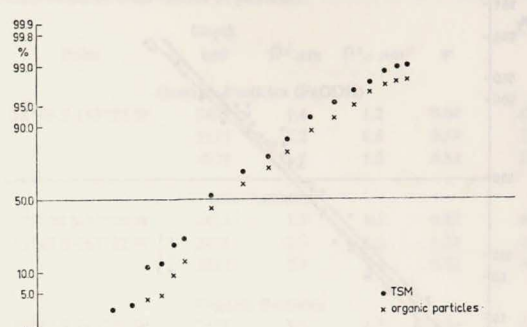

Figure 8. Organic particles and total suspended matter distribution at St. 306, 3879 m.

latter we use a factor of 0.76, after Boido (1947) for square parallelepipedes, with a thickness sufficient to provide the half-sphere volume. We have assumed an *in-situ* ρ_p for suspended aluminosilicate particles of 1.6 g/cm^3, a value proposed by Gardner *et al.* (1976) for nepheloid layer material, in order to determine a maximum flux. Higher in the water column most aluminosilicate particles have associated organic matter which reduces their effective density. The aluminosilicate fluxes were calculated for various stations and depths in intermediate and deep waters. We have used the same approach to calculate the flux of aluminosilicate due to settling of the larger aggregate particles. These grains are very open and organic-rich, and we have assumed a ρ_p of 1.06 g/cm^3. A value of 20% of aluminosilicate in these aggregates was used, once again, to obtain maximum values for the flux. The calculated fluxes yield an estimate of 10-30 μg/cm^2/yr.

Mean settling velocity and residence time $\bar{t}$ for these particles are calculated from the fluxes using:

$$\bar{w} = \frac{\Phi}{M} \quad \text{where } \bar{w} = \text{mean settling velocity, } \Phi = \text{total flux and } M = \text{total mass concentration}$$

For individual aluminosilicate particles the settling rates range between 30 and 150 m/yr, and for the aggregates, between 300 and 600 m/yr. The mean residence time of individual aluminosilicate particles is calculated as ~ 100 years, and that for aggregates as ~ 20 years .The mixed population of these two categories have a combined mean residence time of ~ 80 years in the intermediate waters.

This indicates that the transport of individual aluminosilicate particles in the intermediate waters is mainly controlled by advective processes. Such particles are maintained within the water column by the general ocean circulation (Chesselet, 1975; Brun-Cottan, 1976a). The long residence times explain the very low combined fluxes (10-30 $\mu g\ cm^{-2}yr^{-1}$), which account for only a few percent of the total accumulation of aluminosilicates in deep sea sediments (0.2-1.2 mg $cm^{-2}\ yr^{-1}$, Ku *et al.*, 1968; Turekian, 1965). As our calculations were deliberately made to attain the maximum values of fluxes, this discrepancy cannot be accounted for by the uncertainties on the different parameters we used.

Meanwhile, it has been recently shown that the main carrier of aluminosilicates is the large fecal aggregates driving a flux which can account for 30 to 50% of the global sedimentation rate of aluminosilicates (the fecal material can only be observed in large-volume filtrations: Bishop *et al.*, 1977, 1978; and sediment traps: Spencer *et al.*, 1978). This, together with near bottom horizontal mass transport of material from the continental margins, provide the bulk of sedimentary aluminosilicates.

9. Discussion

The results provide a first order indication of the size distribution of individual aluminosilicates in the ocean. They all follow log-normal functions with a limited range of mean diameter and standard deviation. Such similarity amongst samples from many different geographic locations has already been observed for total suspended matter examined by Coulter counter (Lerman *et al.*, 1977; Brun-Cottan, 1976a,b). The world-wide similarity of the size distributions we observe for aluminosilicate particles in the open ocean is remarkable. The variability of input mechanisms and sources are not reflected in the ocean. We view this as the end result of the whole set of transport phenomena affecting the particles, which tend to create a uniform size distribution.

The log-normal size distribution we observe for oceanic aluminosilicate particles is not unusual, considering that such particles are virtually inert chemically and that scientists have observed such patterns in sediments for decades (e.g. Krumbein, 1938; Rogers and John, 1959; Spencer, 1963; Brun-Cottan, 1967). Indeed, the size distribution of detrital grains can be cited as a classic example of log-normal functions (Aitchinson and Brown, 1976).

It is notable, however, that the reactive components we have measured, silica, Fe-oxides and to some extent organic particles, also fit a log-normal distribution. The same has recently been shown for $CaCO_3$ debris and for $BaSO_4$ (see introduction). Together with the aluminosilicates, these represent virtually all of the major components of suspended matter.

These results run counter to many previously published studies of total suspended matter (Bader, 1970; Brun-Cottan, 1971, 1976a,b; Wellershaus *et al.*, 1973). Can

the sum of a set of log-normal components (total) be a power function? The few examples we have of counts of all components do not suggest this at all. A power model requires that there be very large numbers indeed of very fine particles and these have not been observed with the scanning electron microscope down to 0.2 μm. Nor have they been detected by the Coulter counter method (which gave rise to the belief in a power function) because technical difficulties have prevented the counting of particles finer than about 1-2 μm. It is precisely just below this size that the SEM data reveal the rapid departure from continued increase in particle numbers. The peak in the gaussian distribution is just at the lower limit of published size analyses and these have thus seen only a part of the distribution. Because of this, there has been a certain tendency in the literature to ignore the signals in the data that argued against a power distribution. Thus in the treatment by Wellershaus *et al.* (1973) an apparent peak at about 2 μm is ignored in order to preserve a straight line power function, and power parameters are used in Bishop *et al.* (1978) to describe histograms which show a very gaussian form, even for relatively coarse particles. Fukuda (1974), however, assumed a log-normal particle size distribution and discussed its implications.

The only published study, including sizes of marine particles finer than 1 μm, which shows a power distribution is that of Gulf of Mexico suspended matter. Harris (1977) examined total suspended matter using a transmission electron microscope and was not able to ascertain the chemistry of the particles he had counted. We have specifically examined the deep water filters with a transmission electron microscope and compared the fields with the image obtained by scanning electron microscope. No particles were present on the transmission image which were not on the scanning image. Our SEM-EMP detection limit was 0.1 μm rather than the 0.02 μm optical limit of Harris. We have, however, not found particles finer than 0.4 μm in any abundance on the GEOSECS Nuclepore filters examined in the present study.

10. Conclusions

An approach combining scanning electron microscopy, electron microprobe analysis, and instrumental neutron activation analysis, shows that individual aluminosilicate particles from intermediate and deep ocean waters fit a log-normal distribution. The distribution curves for such particles vary only slightly from place to place in the ocean. The same appears to be true for aggregate particles. A distinct form of aggregate particles, rich in aluminosilicate, characterizes the bottom nepheloid layer.

Log-normal size distributions are observed as well for silica, iron oxides and hydroxides and organic particles, and have also been reported for calcium carbonate debris and barite particles. These distributions reflect a population of particles with long residence times.

The flux of fine particles of aluminosilicates studied here is about 10-30 $\mu g/cm^2$/yr and accounts for a few percent of the flux of aluminosilicates to the sea floor. Other sources, very probably the much larger, fast-settling fecal material, and near-bottom horizontal mass transport of material from the continental margins, provide the bulk of sedimentary aluminosilicates.

Acknowledgments. We would like to thank the GEOSECS Operation Group which provided samples of oceanic suspended matter from the GEOSECS expedition. We acknowledge P. Biscaye, P. Buat-Menard, R. A. Duce, J. C. Duplessy, D. Lal, I. N. McCave for helpful comments and suggestions and J. Klossa for his assistance in the analyses of the filters. We are grateful to "Pierre Süe Laboratory" at Saclay, where we performed the neutron activation analyses.

REFERENCES

Aitchison, J. and J. A. C. Brown. 1976. The Lognormal Distribution With Special Reference to Its Uses in Economics. Cambridge Univ. Press.

Aubey, O. 1976. Contribution à l'étude de la dissolution des particules de carbonate de calcium dans les eaux profondes océaniques. Thèse de 3e Cycle, Univ. Pierre et Marie Curie, Paris 6.

Aubey, O. and R. Chesselet. 1977. Distribution of suspended coccoliths and $CaCO_3$ debris in the Central Argentine Basin. AGU, Spring Annual Meeting, Abstract EOS Trans. AGU.

Bader, H. 1970. The hyperbolic distribution of particle sizes. J. Geophys. Res., *75*, 2822–2830.

Bishop, J. K. B., J. M. Edmond, D. R. Ketten, M. P. Bacon and W. B. Silker. 1977. The chemistry, biology and vertical flux of particulate matter from the upper 400 m of the Equatorial Atlantic Ocean. Deep Sea Res., *24*, 511–548.

Bishop, J. K. B., D. R. Ketten and J. M. Edmond. 1978. The chemistry, biology and vertical flux of particulate matter from the upper 400 m of the Cape Basin in the Southeast Atlantic Ocean. Deep Sea Res., *25*, 1121–1161.

Boido, J. 1947. Etude de la vitesse de chute des particules lamellaires et aciculaires. Cited by Brun-Cottan, 1976b.

Boyle, E. A., F. R. Sclater and J. M. Edmond. 1977. The distribution of dissolved copper in the Pacific. Earth Planet. Sci. Lett., *37*, 38–54.

Brewer, P. G., D. W. Spencer, P. E. Biscaye, A. Hanley, P. L. Sachs, C. L. Smith, S. Kadar, J. Fredericks. 1976. The distribution of particulate matter in the Atlantic Ocean. Earth Planet. Sci. Lett., *32*, 393–402.

Bruland, K. W., G. A. Knauer and J. H. Martin. 1978. Zinc in North-East Pacific water. Nature, *271*, 741–743.

Brun-Cottan, J. C. 1967. Influence du marquage radioactif sur les paramètres dynamiques des sédiments pélitiques. Thèse de Spécialité, Paris.

—— 1971. Etude de la granulométrie des particules marines. Mesures effectuées avec un compteur Coulter. Cahiers Océanographiques, *23*, 193–205.

—— 1976a. Stokes settling and dissolution rate model for marine particles as a function of size distribution. J. Geophys. Res., *81*, 1601–1606.

—— 1976b. Contribution à l'étude de la granulométrie et de la cinétique des particules marines. Thèse de Doctorat d'Etat, Paris.

Buat-Ménard, P. and R. Chesselet. 1978. Marine aerosols control on deep ocean heavy metals particulate chemistry. Proc. 9th Intern. Conf. on Atmospheric Aerosols, Condensation and Ice Nuclei, Galway (Ireland). Pergamon Press (in press).

—— 1979. Variable influence of the atmospheric flux on the trace metal chemistry of oceanic suspended matter. Earth Planet. Sci. Lett., *42*, 399.

Chesselet, R. 1975. Deep suspended matter chemistry. Thalassa Jugoslavica, *11,* 135–138.

Dehairs, F., R. Chesselet and J. Jedwab. 1980. Discrete suspended particles of barite and the barium cycle in the open ocean. Earth Planet. Sci. Lett., *49,* 528–550.

Fukuda, M. 1974. Vertical diffusion of suspended particles from the sea bottom. J. Ocean. Soc. Japan, *30,* 67–76.

Gardner, W. D., C. D. Hollister, D. W. Spencer and P. G. Brewer. 1976. Characteristics of near-bottom suspended sediments of the Northeastern Atlantic. Abstract EOS Trans. AGU, *57,* 269.

Harris, J. E. 1977. Characterization of suspended matter in the Gulf of Mexico-II. Particle size analysis of suspended matter from deep water. Deep Sea Res., *24,* 1055–1061.

Junge, C. E. 1963. Air chemistry and radioactivity, Academic Press, New York.

Krumbein, W. C. 1938. Size distributions of sediments and the Normal Phi Curve. J. Sed. Petr., *U18,* 84–90.

Ku, T. L., W. S. Broecker and N. Opdyke. 1968. Comparison of sedimentation rates measured by paleomagnetic and the ionium methods of age determination. Earth Planet. Sci. Lett., *4,* 1–16.

Lambert, C. E. 1979. Contribution à l'étude du fer et de l'aluminium particulaires dans l'océan, DES, Université de Picardie.

Lerman, A., K. L. Carder and P. R. Betzer. 1977. Elimination of fine suspensoids in the oceanic water column. Earth Planet. Sci. Lett., *37,* 61–70.

Rogers, J. and J. W. John. 1959. Detection of log normal size distributions in plastic sediments. J. Sed. Pet., *29,* 402–407.

Sclater, F. R., E. Boyle and J. M. Edmond. 1976. On the marine geochemistry of nickel. Earth Planet. Sci. Lett., *31,* 119–128.

Spencer, D. W. 1963. The interpretation of grain size distribution curves of plastic sediments. J. Sed. Petr., *33,* 180–191.

Spencer, D. W., P. G. Brewer, A. Fleer, S. Honjo, S. Krishnaswami and Y. Nozaki. 1978. Chemical fluxes from a sediment trap experiment in the deep Sargasso Sea. J. Mar. Res., *36,* 493–523.

Turekian, K. K. 1965. Some aspects of the geochemistry of marine sediments, *in* Chem. Oceanogr., *2,* 81–126.

—— 1977. The fate of metals in the oceans. Geochim. Cosmochim. Acta, *41,* 1139–1144.

Wellershaus, S., L. Göke and P. Frank. 1973. Size distribution of suspended particles in sea water. Meteor. Forsch. Ergebnisse, *16,* 1–16.

Received: *13 December, 1979;* revised: *26 September, 1980.*